ORIGINAL RESEARCH PAPER

Modeling of adsorption isotherms and competitive adsorption breakthroughs of Nicotine/Pyridine removal from aqueous solution by activated Montmorillonite

Zeinab Ibrahim[1,2], Yehya Mohsen[1], Joumana Toufaily[2], Wassim Rammal[3], Tayssir Hamieh[1], T. Jean Daou[4], Maria-Laura Foddis[5] and Bachar Koubaissy[2*]

[1] *Laboratoire Matériaux, Catalyse, Environnement et Méthodes Analytiques (MCEMA), EDST, FS, Université Libanaise, Campus Hariri, Hadath, Beyrouth, Liban.*

[2] *Laboratoire des Etudes Appliquées au Développement Durable et Energie Renouvelable (LEADDER), EDST, Université Libanaise, Campus Hariri, Hadath, Beyrouth, Liban*

[3] *Université Libanaise, Faculté des sciences V, Nabatieh, Liban*

[4] *Université de Strasbourg, Université de Haute Alsace, Axe Matériaux à Porosité Contrôlée (MPC), Institut de Science des Matériaux de Mulhouse (IS2M), UMR CNRS 7361, ENSCMu, 3 bis rue Alfred Werner, 68093 Mulhouse Cedex, France.*

[5] *DICAAR-Dipartimento di Ingegneria Civile Ambientale e Architecttura, Università de Cagliari, Italia*

ABSTRACT

Activated Montmorillonite (AM) reveals as a low-cost and efficient adsorbent for the adsorption of nicotine and pyridine from aqueous solutions. In this study, the influence of several operation conditions (initial compounds concentration, volumetric flow rate, and height of bed) on the shape of breakthrough curves and the mass transfer resistance was evaluated. Adsorption experiments were developed to determine the adsorption isotherm of the system, then the adsorption of pyridine and nicotine onto activated Montmorillonite in single and binary systems has been studied using fixed-bed adsorption column. In continuous adsorption, Results show that the maximum nicotine uptake 0.68 mmol/g of AM was achieved through electrostatic attraction and hydrogen bond at a pH = 6.3, a flow rate of 1 ml/min and a height of bed equal to 12 mm. In binary mixtures, zeolite adsorption is governed primarily by the size of pollutants present in water. Thus, the bigger compound (in this case, Nicotine), was adsorbed more easily than the pyridine present in the mixture. Experimental data were fitted according to Fowler Guggenheim for the isotherms and Wolborska model for the breakthroughs. AM was regenerated by ethanol and the results show that about 94% of the adsorption capacity is maintained after three times of cyclic adsorption-desorption process.

Keywords: *Adsorption, Nicotine, Pyridine, Fixed-Bed Column, Activated Montmorillonite*

INTRODUCTION

The presence of nicotine and its derivatives in wastewaters are originated from industrial, agricultural, and human activities [1-3]. Many of these compounds are used every day as consumer products and by-products [4, 5]. Each year, more than 500 billion tons of nicotine-containing wastewater is released globally [6]. Moreover, wastewaters also contain significant concentrations of polycyclic aromatic hydrocarbons PAHs (up to 30 mg/L). These compounds are investigated as priority pollutants as they are durable persistent and highly mobile over the environment. Also, many of them can inhibit the biological process. All of these compounds need special attention because of their high toxicity for the environment and society [7, 8].

Numerous methods have been used for the

removal of these kinds of pollutants from the environment, including advanced oxidative process [9], photocatalytic degradation [10] and ozonation [11] but each treatment has its constraints in terms of feasibility, efficiency, practicability, reliability, environmental impact, sludge production, pre-treatment requirements and the formation of potentially toxic by-products. Adsorption techniques represent the most desired easy way to remove inorganic and organic pollutants [12-14], therefore adsorption is technologically simple (simple equipment) and adaptable to many treatment formats and applicable to a wide range of commercial products and highly effective process with fast kinetics and excellent ability to separate a wide range of pollutants.

The selected adsorbents must demonstrate in most of the cases a large specific surface area and excellent affinity to the pollutants to be adsorbed. Among natural materials, activated carbon, zeolites and clay minerals are commonly used for the treatment of water. Activated carbon has excellent adsorption properties for many organic products; although its use is rather limited due to its expensive cost [15-16] and its harmful effects on the environment because it is partially regenerated so spent adsorbent may be considered hazardous waste.

Recently, research is focused on new, efficient, low-cost, and easily accessible natural materials such as clay materials, to be used as adsorbents [17-20] due to the heterogeneity of their surfaces. Montmorillonite is a type of clay mineral that has been used as non-biomaterials for the purification of pharmaceutical wastewater. The results show that Montmorillonite is an effective sorbent to remove ciprofloxacin [19], and pyridine [21] from water. Further, Montmorillonite has been demonstrated to have a high adsorption capacity for tetracycline (TC) [22]. The mechanism was referred to intercalation of these molecules into the interlayer space of Montmorillonite. The adsorption capabilities of natural clay are attributable to their high surface area and exchange capacities, including the presence of negative charges on the clay mineral structure [20]. Li et al confirmed by quantitative correlation between cations desorbed and protonated tetracycline adsorbed that cation exchange was the main mechanism for TC adsorption over smectite [22]. On the other hand, Ibrahim et al showed that the adsorption of pyridine over activated Montmorillonite had occurred by physical interactions as hydrogen bond interactions [21].

Most previous research using Montmorillonite for adsorption is based on batch kinetic and batch equilibrium studies. Fixed bed column adsorption has been in general used to remove many organic compounds from aqueous solution [23-25]. But the optimization of adsorption operating conditions and industrial design demanded considerable financial resources. The significant breakthrough curves for a specific adsorption process are fundamental when determining the operating parameters such as the feed flow rate and the influence of the concentration of the solutions [26]. The optimization of fixed-bed column involves mathematical models that are used for the description of the breakthrough curves [27].
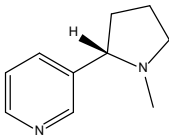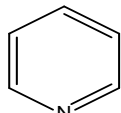
Presently, according to our knowledge, very little study exists on the activated Montmorillonite as a sorbent for the removal of toxic molecules on a fixed-bed adsorption column. The main objective of the present work is to explore the performance of the Activated Montmorillonite (AM) as an adsorbent for the removal of toxicant compounds such as nicotine and pyridine from aqueous solution. In this paper, the removal efficiencies were conducted in batch and flow apparatuses on single-component solutions and mixtures. The effects of the solution pH and molecule size were studied, as well as the effects of the flow rate and bed height on the breakthrough curves. This present work is devoted also to the kinetic study of the adsorption of these toxic molecules onto AM in a fixed-bed column experiment as well as by mathematic modeling. The analytical breakthrough curve model of Wolborska [28, 29] was used and the model was verified by comparing the experimental and the prediction results. Lastly, the regeneration and reuse of Montmorillonite also were presented.

MATERIALS AND METHODS
Reagents
Nicotine and pyridine were supplied from Sigma Aldrich in analytical purity and were used to prepare different concentrations of each solution. The physical and chemical properties of each compound are shown in Table 1. A Commercial Montmorillonite (MK10) was used and was activated with sulfuric acid (0.5 M), then washed by water to remove the excess of the H^+. This step was followed by drying at 105°C for 24h and then selected by sieving in a size fraction between 2.00 and 4.00 mm.

J. Water Environ. Nanotechnol., 5(2): 114-128 Spring 2020

115

Table 1. Physical and chemical properties of nicotine and pyridine.

Adsorbates	Chemical structure	Octanol/water partition coefficient log Kow	Wavelength (nm)	Kinetic diameter (Å)	Solubility (mg/L)	pka
Nicotine		1.17	260	7.8	1×10^6	pKa$_1$=3.04 pKa$_2$=7.84
Pyridine		0.65	256	6	1.1×10^6	pKa =5.23

Analytical methods

The concentration of all samples was determined by UV-Vis spectrophotometer for the mono-compounds and by HPLC for the binary mixture compounds. All samples were centrifuged before the analysis to eliminate the interference of the clay in the analysis. The samples were analyzed by spectrophotometry (Hitachi-U-2900 Spectrophotometry) for the monocompounds or by HPLC (VWR Hitachi Autosampler L-2200) techniques to measure the amount of each compound in a binary mixture solution. A C18 column was used and maintained at a temperature of 35°C. The chemical separation was achieved by a mobile phase consisting of acetonitrile (ACN)-sodium hydrogen carbonate (pH 10.0, 0.03M) (20:80, v/v), at a flow rate of 1 ml/min. The UV detection was achieved at a wavelength equal to 259 nm.

Characterization techniques

Zeta potentials of activated Montmorillonite samples were measured at 22˚C ± 1˚C using a Zeta Meter 4.0 equipped with a microprocessor unit (PRASE-EDST, LU, Lebanon) (Table 2).

The mobility is negative as observed in Table 2. This indicates that the AM is negatively charged at various pH ranges (2 to 11).

FT-IR study was carried out using the FTIR-6300 apparatus from JASCO (PRASE-EDST, LU, Lebanon). FTIR spectra were recorded in the range of 400 - 4000 cm^{-1} at a resolution of 4 cm^{-1} with KBr pellets method. No much variation of the absorption bands in Montmorillonite clay after its activation with acid, so the acidification treatment does not affect the crystalline structure of the Montmorillonite (Fig. SD1).

X-ray diffraction patterns were obtained for powder samples, using a D8 Bruker X-ray diffractometer (copper anticathode of wavelength λ Kα = 0.154060 nm; PRASE-EDST, LU, Lebanon). The XRD patterns of the samples given in Fig. SD2 shows that no significant difference between the XRD patterns of activated clay with that of the untreated Mt clay.

The microporous and mesoporous volumes and the specific surface area (Table 3 and Table SD1) were determined using the nitrogen adsorption-desorption isotherms performed at −196˚C on a Micromeritics ASAP 2420 apparatus (IS2M, UHA, France). The surface area was calculated according to the BET method. The microporous volumes (V_{micro}) were calculated using the t-plot method. The pore size distribution was determined by using the Barrett–Joyner– Halenda (BJH) model applied to the desorption branch and the Density Functional Theorie (DFT) model applied to the adsorption

Table 2. Zeta potential (ζ) of Activated Montmorillonite as a function of pH, at 25˚C.

pH	2	4	7	9	11
ζ (mV)	-38.77	-63.32	-78.08	-106.2	-105.8

Table 3. Porous characteristics of activated Montmorillonite AM.

Abbreviation	AM
SBET (m^2/g)	216
Microporous volume (cm^3/g)	0.04
Mesoporous volume (cm^3/g)	0.26
Pores Diameter (nm)	5.4

116

J. Water Environ. Nanotechnol., 5(2): 114-128 Spring 2020

branch. The total pore volume was calculated at $p/p^o = 0.9$. The results obtained are presented in Figs. (SD3, SD4, and SD5). The adsorption-desorption isotherms of activated montmorillonite with an apparent hysteresis loop, indicative of the existence of defined mesopores in the frameworks (SD3).

We can see from these results that the acid treatment does not affect the crystalline structure of the Montmorillonite, so there is a change just in the site density and surface acidity of Montmorillonite.

Adsorption Methods
Batch adsorption method

The experimental isotherms for the organic compounds, from distilled aqueous solutions on Activated Montmorillonite, were measured at 298 K and different pH. The pH of the solution was adjusted using 0.1 M HCl or NaOH solutions. The effect of pH was studied at pH equal to 2.2, 6.3, and 9.5.

For each equilibrate isotherm, 20 mg of the adsorbent was added to 10 mL of solution (e.g., nicotine or pyridine concentrations of 10, 25, 50, 100, 250, 500, and 1000 mg/L) to reach equilibration in 24h in batch equipment.

The adsorbed amounts are calculated by equation 1:

$$m_A (Q) = V (C_0 - C) \tag{1}$$

Where m_A is the mass of AM (g), V is the volume of solution (L), C is the concentration after adsorption (mmol/L), C_0 is the initial concentration (mmol/L), and Q is the adsorbed amount (mmol/g of AM).

Fixed bed column studies

Fixed bed experiments were carried out using a stainless steel column of 1.8 cm internal diameter and 8 cm of total length. The desired solutions were pumped in up-flow mode through the column at a controlled flow rate using a Gilson pump (model 307) as shown in Fig. 1. Adsorbent, AM, was load in the column and the amount was adjusted, filling it with glass marbles to complete the volume and avoid the dead volume. The column was closed and the samples were collected. For each experiment different volumes of inlet effluent that depended on the individual experiment's saturation time were used. All experiments were performed at room temperature using distilled water. This fixed-bed column was maintained at temperature 25°C with a thermostatic bath.

Theoretical model
Batch adsorption method

The adsorption of organic compounds on activated Montmorillonite adsorbents takes place in aqueous phase with or without variation of the pH of the solution. However, the use of a single-component model has been successfully used to describe the adsorption of the organic compound. The Fowler and Guggenheim [30] model follow the equation 2:
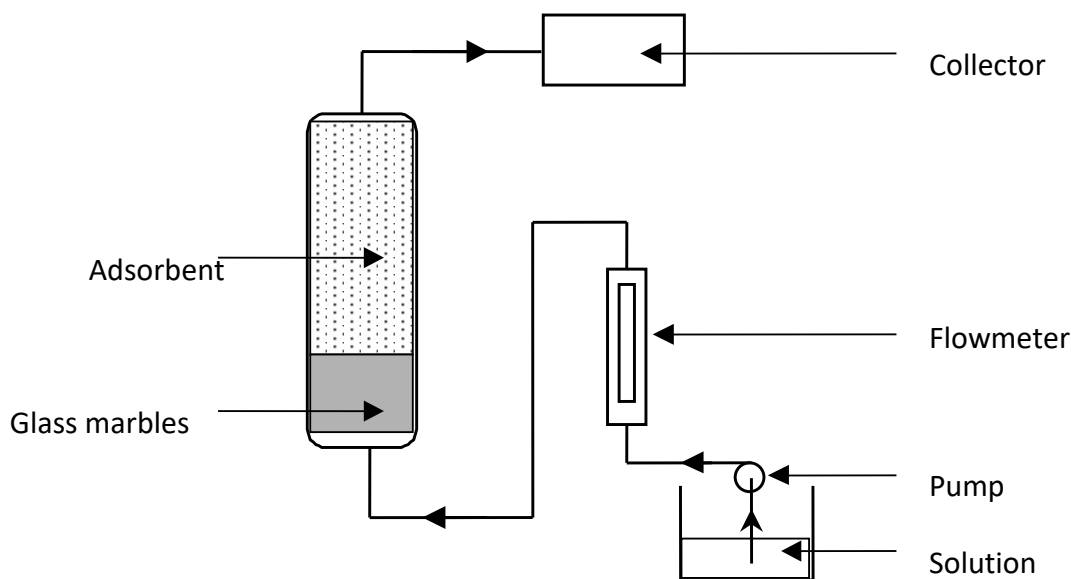

Fig. 1. Diagram of the adsorption system under dynamic conditions.

J. Water Environ. Nanotechnol., 5(2): 114-128 Spring 2020

117

$$KC = \frac{\theta}{1-\theta} \exp\left(\frac{2\theta W}{RT}\right) \qquad (2)$$

where K is the equilibrium constant for the adsorption of the adsorbate on an active site (L/mol); C is the concentration at the equilibrium adsorption (mol.L^{-1}); W is the empirical interaction energy between two molecules adsorbed on nearest neighboring sites (J. mol^{-1}); R is the ideal gas constant (8.314 J.mol^{-1}.K^{-1}); T is the thermodynamic temperature (K), and θ is the fractional coverage of the surface.

Fowler Guggenheim's equation is one of the simplest equations taking into account the lateral interactions. This model is based on the hypothesis that interaction energy is constant and independent of the surface fractional coverage θ, and hence independent of the number and the distribution of the adsorbed molecules.

Fixed bed column

The empirical equation proposed by Wolborska was used to describe the breakthrough curves in a fixed bed column [25, 26]. This model is based on the general equation of mass transfer for the diffusion mechanism for a low concentration range of breakthrough curves. The mass transfer in the fixed bed adsorption is described by the following equations

$$\frac{dC_{ix}}{dt} + u\frac{dC_{i_x}}{dx} + \frac{(1-\varepsilon)}{\varepsilon}\frac{da}{dt} = D_{ax}\frac{d^2C_{i_x}}{dx^2} \qquad (3)$$

Where C_{ix} is the solute concentration in the bulk solution and D_{ax} is an axial diffusion coefficient, x is bed depth, u is linear flow velocity, a is removal capacity, ε is extra-granular porosity of bed.

The solution of differential equation gives equation 4. The Wolborska model follows this equation:

$$\ln\frac{C}{C_0} = \frac{\beta C_0}{Q_{ads}}t - \frac{\beta}{u}h \qquad (4)$$

With

$$\beta = \frac{u^2}{2D_{ax}}\left(\sqrt{1 + \frac{4\beta_0 D_{ax}}{u^2}} - 1\right) \qquad (5)$$

Where C_0 is the initial concentration of pollutant (mol/L); Qads is the concentration of pollutant in the adsorbent (mol/g); β_0 is the external mass-transfer kinetic coefficient (min^{-1}); h is the height of the adsorbent bed (cm), and u is the flow rate of the pollutant solution (mL.min^{-1}).

The β coefficient, which is not constant in our case and it is determined from the breakthrough curve, represents the interaction between the adsorbate and the adsorbent:

β = a. Q$_{ads}$/C$_0$, where a represents the slope of the curve (interaction strength between the adsorbate and the adsorbent), Q$_{ads}$ is the quantity of pollutant adsorbed at the equilibrium, and C$_0$ is the initial pollutant concentration. For saturation capacity we use Q$_{max}$.

In a previous work [12], this model has been used to describe the entire curve.

For competitive adsorption, the breakthrough of the non-desorbed compound has a form similar to a compound absorbed without competition. To describe the breakthrough curve of the desorbed compounds, the model below is proposed whose different terms are taken from wolborska model

$$\frac{C_2}{C_m} = \left(\frac{e^{\frac{\beta_a C_{2,0}}{a_{2,0}}}}{e^{\frac{\beta h}{u}}}\right)_{0 \prec t \prec t_{1/2}} + \frac{1}{e^{\frac{\beta_a h}{u}}}\left[2e^{\frac{\beta_a C_{2,0}}{a_{2,0}}t_{1/2}} - e^{\frac{\beta_a C_{2,0}}{a_{2,0}}(2t_{1/2}-t)}\right]_{t_{1/2}\prec t \prec \infty}$$

$$-(C_m-1)\left(\frac{e^{\frac{\beta_a C_{1,0}}{a_{1,0}}t}}{e^{\frac{\beta h}{u}}}\right)_{0 \prec t \prec t'_{1/2}}\frac{C_2}{C_1} \qquad (4)$$

$$-(C_m-1)\frac{1}{e^{\frac{\beta_a h}{u}}}\left[2e^{\frac{\beta_a C_{1,0}}{a_{1,0}}t'_{1/2}} - e^{\frac{\beta_a C_{1,0}}{a_{1,0}}(2t'_{1/2}-t)}\right]_{t'_{1/2}-t}\frac{C_2}{C_1}$$

Where $C_{1,0}$ is the initial concentration of non-desorbed compound; $C_{2,0}$ is the initial concentration of desorbed compound; C_m is the maximal concentration of desorbed compound; $a_{1,0}$ is the concentration in the adsorbent of the desorbed compound; $a_{2,0}$ is the concentration in the adsorbent of the non-desorbed compound; $t_{1/2}$ is the average time of stay of the non-desorbed compound in the adsorbent, and $t'_{1/2}$ is the average time of stay of the desorbed compound in the adsorbent.

RESULTS AND DISCUSSION
Influence of pH on the adsorption of nicotine

The adsorption capacity at different pH and different concentrations are presented in Fig. 2 and Fig. SD6. The results show that the best adsorption is obtained at pH = 6.3. Nicotine has two pKa values: 3.04 and 7.84, At pH= 6.3, Nicotine is

118

J. Water Environ. Nanotechnol., 5(2): 114-128 Spring 2020

predominantly found in its monoprotonated form and it is adsorbed over AM by H-bond between the oxygen of the AM and the hydrogen of the NH-group. Then, we observed a decrease in the adsorption capacity at pH = 2.2 and pH = 9.5.

In an acidic medium (pH = 2.2), the decrease can be explained by the formation of hydronium ions (H_3O^+), which can interact with the negative sites of the activated Montmorillonite (O^{2-}), leading to a concurrence between the H_3O^+ ions and the diprotonated species of nicotine. This conducts to a weaker interaction between the nicotine and the negative sites.

Whereas at pH=9.5, Nicotine is found mostly in its molecular. The decrease of the adsorption amount at this pH is explained by the less acidic character of nicotine which leads to lower adsorption with the basic O^{2-} sites of the Montmorillonite. Similar results were obtained by Koubaissy et al for adsorption of phenol drifts on 3

zeolites and Ibrahim et al for adsorption of pyridine on Activated montmorillonite [21, 31].

Effect of flow rate on nicotine adsorption onto activated Montmorillonite.

The adsorption of nicotine as a function of flow rates over 2 g of activated Montmorillonite was studied. The breakthrough curves corresponding to these adsorptions on activated Montmorillonite and their modeling according to the Wolborska model are shown in Fig. 3.

It can be seen that for a flow rate of 1 mL/min, 1.5 mL/min, and 2 mL/min, the elution volumes V_0 are respectively equal to 130 mL, 50 mL, and 20 mL. This result shows that the breakthrough curves are highly affected by the feed flow rate. On the other hand, for the same concentration of the solution, we observe that the value of the coefficient β (Table 4), which reflects the adsorbent-adsorbate interaction, is higher for a flow rate of 1 mL/min.
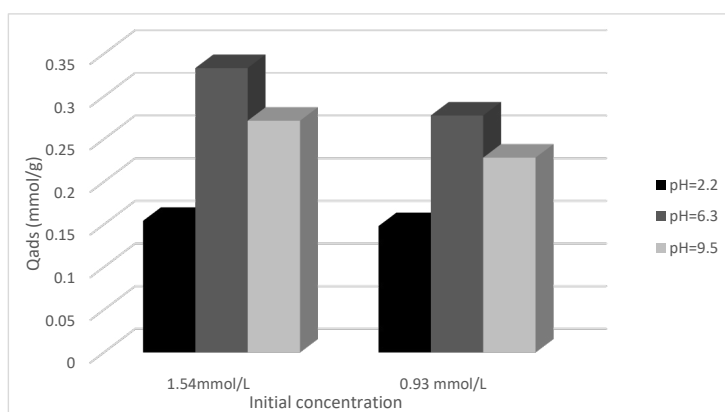

Fig. 2. Adsorption capacity of activated Montmorillonite (AM) at different pH and different initial concentration of nicotine.
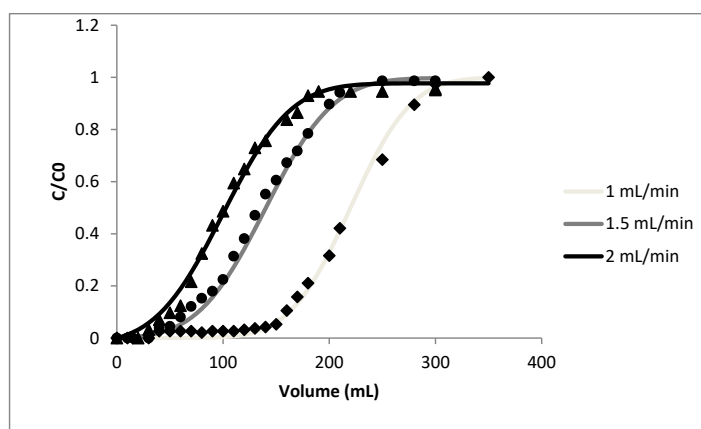

Fig. 3. Breakthrough curves of nicotine (0.25g/L) onto AM obtained at different volumetric flow rates.

J. Water Environ. Nanotechnol., 5(2): 114-128 Spring 2020

119

Meng et al. [32] showed that shorter Breakthrough times were observed at higher flow rates. In fact, at these flow rates, and according to Chen et al. [33], the residence time in the column is usually not long enough. So, an adsorbate molecule leaves the column before reaching the adsorption equilibrium. The Wolborska model was also used to fit the breakthrough curves. As seen from Table 5, the root mean squared errors RMSE were determined, the values obtained which are lower than 5% indicate that the breakthroughs of all flow rates are very well described by this model.

Effect of bed height on breakthrough curve

In the present investigation, the effect of bed height on the nature of breakthrough curve is studied for 4 different bed heights. It is noticeable from Table 5, using a constant influent concentration of 6.2mmol/L and a flow rate of 1 ml/min. The breakthrough time increases with increasing bed height. This happens because, at higher bed height, nicotine remains in contact with the adsorbent for a longer duration, thus resulting in higher adsorptive capacity. A higher bed height indicates a larger amount of adsorbed nicotine due to an increase in the surface area of adsorbent, providing more binding sites for the adsorption.

Similarly, the removal percentage decreases with decreasing bed depth [34].

We can see in Fig. 4 and Table 5, that the shape and the slope of each curve are different from the variation of the bed heights. The breakthrough time and $V_{1/2}$ which is the filtered volume at half-height, increase at higher bed depth of adsorbent. As the bed height is increased from 4 to 16 mm, a decrease in the slope of the breakthrough curve is observed, which resulted in a rapid mass transfer zone.

Effect of the concentration of the solution on nicotine adsorption onto activated Montmorillonite

The adsorption of nicotine in an aqueous solution with a concentration ranging from 1.54 mmol/L to 6.2 mmol/L and at a flow rate of 1 mL/min was also studied on the AM. The objective is to compare the effect of the variation in the concentration of the solution on the amount of adsorption. The breakthrough curves corresponding to these adsorptions on activated Montmorillonite and their modeling according to the Wolborska model are shown in Fig. 5.

The β values for the three concentrations are reported in Table 6. It should be noted here that for the different nicotine concentrations of the solution,

Table 4. Parameter values for the breakthrough curves for the adsorption of nicotine for the three different flow rates.

Flow (mL/min)	1	1.5	2
C_0 (mmol/L)	1.54	1.54	1.54
a	0.0062	0.0062	0.0061
a_0 (mmol/g)	0.32	0.22	0.15
β (min^{-1})	1.29	0.88	0.61
RMSE	0.026	0.026	0.03

Table 5. Parameter values for the breakthrough curves for the adsorption of nicotine for the four different bed heights.

Bed height (mm)	4	8	12	16
C_0 (mmol/L)	6.2	6.2	6.2	6.2
a	0.048	0.021	0.014	0.012
a_0 (mmol/g)	0.52	0.57	0.62	0.68
V_0 (mL)	3	15	25	40
$V_{1/2}$ (mL)	22	52	77	100
RMSE	0.045	0.035	0.038	0.024

Fig. 4. Effect of bed height on the adsorption of nicotine by AM.

120

J. Water Environ. Nanotechnol., 5(2): 114-128 Spring 2020

the values of the coefficient β, which reflects the adsorbent-organic molecule's interactions, are the same and is in the range of 1.3 min⁻¹. This result shows that the interaction adsorbent-nicotine do not depend on the nicotine concentration.

The breakthrough points appear faster at high concentrations (6.2 mmol/L) than those at 3.1 mmol/L and 1.54 g/L. In fact, at high values of initial concentration, the adsorption sites are filled more efficiently and the saturation of the column is reached more quickly. The same results are obtained by Sabio et al. [35] and Sotelo et al. [36] which show that the gradient concentration has a significant influence on the adsorption rate.

Comparison of the nicotine and pyridine adsorption on activated Montmorillonite

The adsorption of nicotine and pyridine on activated Montmorillonite was studied in batch and dynamic systems. Fig. 6 reports the adsorption isotherms, obtained at a pH equal to 6.3 over AM, of nicotine and pyridine, and their modeling according to Fowler-Guggenheim. Adsorption on AM was favored for nicotine; the maximal adsorption capacity and the K value of nicotine are as great as that for pyridine (Table 7).

Fig. 7 shows the obtained breakthrough curves and their modeling according to the Wolborska model for the same concentrations (0.5g/L) of

Table 6. Parameter values for the breakthrough curves for the adsorption of nicotine at different concentrations on AM.

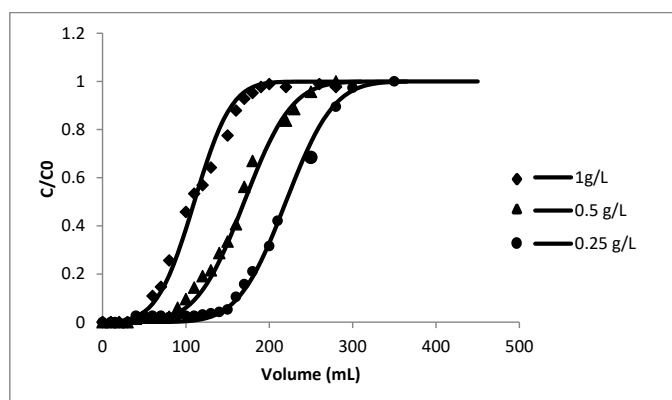| C_0 (mmol/L)	6.2	3.1	1.54
a	0.012	0.0077	0.006
a_0 (mmol/g)	0.68	0.51	0.35
β (min⁻¹)	1.32	1.26	1.35
A (mL/g)	110	164	224
RMSE	0.024	0.03	0.026

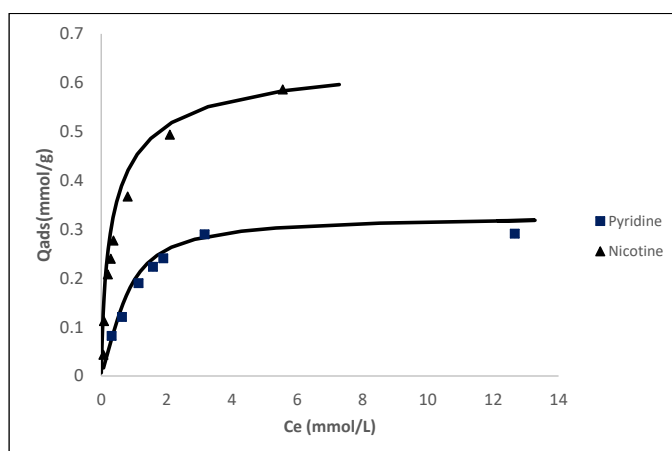Fig. 5. Breakthrough curves of nicotine onto AM obtained at different concentrations.

Fig. 6. Adsorption isotherms of nicotine and pyridine at pH=6.3.

J. Water Environ. Nanotechnol., 5(2): 114-128 Spring 2020

121

Table 7. Parameters values of the Fowler-Guggenheim model from Nicotine and pyridine isotherms obtained for adsorption over AM.

	Nicotine	pyridine
K (L/g)	34	20
Qads (mmol/g)	0.59	0.29

Table 9. Adsorption capacities (mmol/g) obtained by using dynamic and batch technics.

	Dynamic	Batch
Nicotine (6.2mmol/L)	0.68	0.59
Nicotine (3.1mmol/L)	0.53	0.49
Pyridine (6.3mmo/L)	0.35	0.29

Table 8. Parameter values for the breakthrough curves for the adsorption of pyridine and nicotine on AM at equal concentrations.

	Pyridine	Nicotine
C_0 (mmol/L)	6.3	3.1
a	0.017	0.0077
a_0 (mmol/g)	0.35	0.51
β (min^{-1})	0.95	1.26
A (mL/g)	56	164

Table 10. Parameter Values from the Breakthrough Curves of the pyridine/Nicotine (1.58mmol/L /1.54 mmol/L) Mixture in Water with AM.

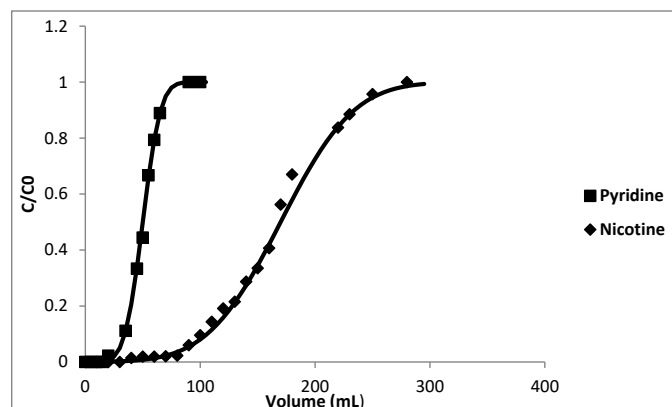|	Pyridine	Nicotine
Ce (mmol/L)	1.58	1.54
qad_{max} (mmol/g)	0.23	-
q_{des} (mmol/g)	0.19	-
q_{ad} (mmol/g)	0.04	0.26
RMSE	0.04	0.03
α (Nicotine/pyridine)	6.5	

Fig. 7. Breakthrough curves of pyridine and nicotine (0.5g/L) onto AM.

pyridine and nicotine, at pH = 6.3 and using 2 g of the adsorbent. The flow rate of the solution was 1 ml/min. The elution volumes V_0 before desorption are 80 mL and 20 mL, respectively. The breakthrough volume of nicotine is greater than that of pyridine, in agreement with the previous results obtained under batch conditions. Therefore, the preferential adsorption of the Nicotine, in comparison with the pyridine, confirms that more-favorable adsorption involves the compound presenting a higher size.

According to Table 8, we observe also that the value of the coefficient β is higher for the nicotine (1.26 min^{-1}) compared to pyridine (0.95 min^{-1}). This could, perhaps, be due to the larger size of nicotine (7.8 Å) compared to pyridine (6 Å). Therefore, there are more available sites for the nicotine molecules to adsorb easily than those

of the pyridine molecules on the mesoporous Montmorillonite. Similar results were obtained by Lu et al [37] for the adsorption of antibiotics onto XAD-4 while the larger molecule presented the largest adsorption amount.

A slight variation between these two techniques is highlighted (Table 9), where we observe an increase in adsorption capacity of 10% when working in dynamic condition, these variations are mainly due to the fact that we work with concentrations outside the equilibrium that differ between the two techniques. And therefore, depending on the shape of the adsorption isotherms, external concentrations can lead to significant differences in terms of adsorption capacity. Van-vilet et al. [38] consider that this difference may come from an unbalanced flow

122

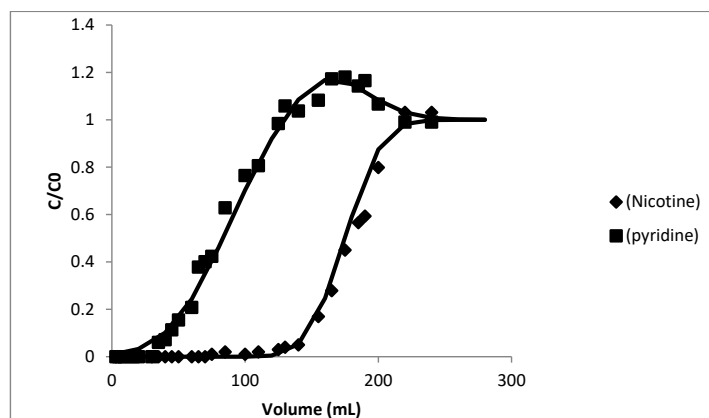*J. Water Environ. Nanotechnol., 5(2): 114-128 Spring 2020*

Fig. 8.   Breakthrough curves of pyridine and nicotine removal (1.58 mmol/L - 1.54 mmol/L) by adsorption onto AM.
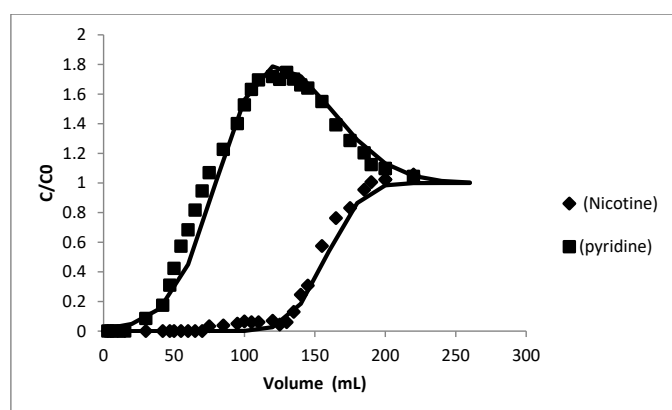

Fig. 9. Breakthrough curves of pyridine and nicotine removal (3.16 mmol/L -1.54 mmol/L) by adsorption onto AM.

system; the diffusion of adsorbates plays a role and can lead to modified flow capacities.

Study of the competitive adsorption of pyridine and nicotine on activated Montmorillonite.

The study reported in this section is focused on the adsorption of the pyridine-nicotine mixture on activated Montmorillonite to highlight the competitive adsorption effects of the two pollutants present in the water. The study was carried out in a fixed-bed column, at atmospheric pressure, at room temperature, at a flow rate of 1 mL/min and a pH = 6.3.

The breakthrough curves of a binary mixture (Pyridine 1.58 mmol/L / Nicotine 1.54 mmol/L) and their modeling according to the modified Wolborska model have been transferred to Fig. 8. It can be seen that nicotine has a conventional breakthrough curve while the shape of the pyridine breakthrough curve is different: it increases to a C/C_0 value close to 1.2 and then decreases to the nicotine breakthrough

curve. This type of curve indicates that after the first adsorption on Montmorillonite, a portion of pyridine is then desorbed. The results are shown in Table 10.

In this case, the pyridine was not adsorbed much in the AM, in comparison to nicotine, which presents the strongest interaction with the adsorbent. Therefore, after 130 mL of solution, AM continues to adsorb Nicotine by eliminating pyridine, and a desorption peak was observed that increased until $C/C0 \approx 1.2$ (see Fig. 8).

Then, the competitive adsorption of pyridine and nicotine from a solution containing this mixture (3.16 mmol/L pyridine/ 1.54 mmol/L nicotine) was studied (Fig. 9).

We notice here the same phenomenon, adsorption-desorption, as above with the value of C/C_0 equal to 1.7. Nicotine is always preferentially adsorbed on activated Montmorillonite. The adsorption capacities of the AM for the nicotine and pyridine have been reported in Table 11.

J. Water Environ. Nanotechnol., 5(2): 114-128 Spring 2020

123

As we see below, Fig. 10 shows the breakthrough curves of pyridine and nicotine removal at concentrations equal to 7.32 mmol/L and 1.54 mmol/L, respectively. It should be noted that whatever the nicotine concentration, the adsorbed amount remains relatively greater (0.246 mmol/g) than that of pyridine (Table 12). But we observe that there is a decrease in the adsorption capacity of pyridine up to 87% in presence of nicotine because the initially adsorbed pyridine is then almost totally desorbed by nicotine. This fact can be interpreted by the high competition between the solutes molecules for the same sites. The solute that has the smaller size (pyridine) was adsorbed firstly then it was desorbed by the largest nicotine which adsorbs more easily on the mesoporous Montmorillonite. Similar results were found in the literature by Lu et al for antibiotics adsorption by porous resins [37].

All the breakthrough curves on adsorbent were experimentally determined and predicted by Wolborska modified model (RMSE ≤5%).

Effect of the adsorption method of nicotine and pyridine molecules over activated Montmorillonite

The values of the selectivity are reported in Tables 10, 11, and 12. We may notice that the ratio

of Henry constants which is equal to the ratio of the slope of isotherms at low concentrations is equal to 1.9 much lower than that of selectivity obtained. Therefore, the evolution from low concentrations to high concentrations increases the adsorption affinity of the nicotine, which is consistent with the type "S" isotherm. This means that adsorbent-adsorbate interaction increases as the concentration increases [39].

To better visualize the effect of the presence of a second adsorbate, we have shown the evolution of the selectivity (α Nicotine/pyridine) as a function of the nicotine molar (%) in Fig. 11. Regardless of the initial percentage in the solution, the adsorption of nicotine is in all cases much greater than that of pyridine and that the separation coefficient is almost always greater than 3. It, therefore, appears that the nicotine has a very high affinity compared to that of pyridine in the case of AM.

Adsorption mechanism

The sorption mechanism of nicotine on activated Montmorillonite has been investigated using FTIR spectroscopy. The different bands in the case of AM alone and AM after adsorption of nicotine are presented in Table 13 and Fig. 12. After the

Table 11. Parameter Values from the Breakthrough Curves of the pyridine/Nicotine (3.16mmol/L /1.54 mmol/L) Mixture in Water with AM.

	Pyridine	Nicotine
Ce (mmol/L)	3.16	1.54
$q_{ad\ max}$ (mmol/g)	0.258	-
$q_{dés}$ (mmol/g)	0.205	-
q_{ad} (mmol/g)	0.053	0.248
RMSE	0.05	0.04
α (Nicotine/pyridine)	4.67	

Table 12. Parameter Values from the Breakthrough Curves of the pyridine/Nicotine (7.32mmol/L / 1.54 mmol/L) Mixture in Water with AM.

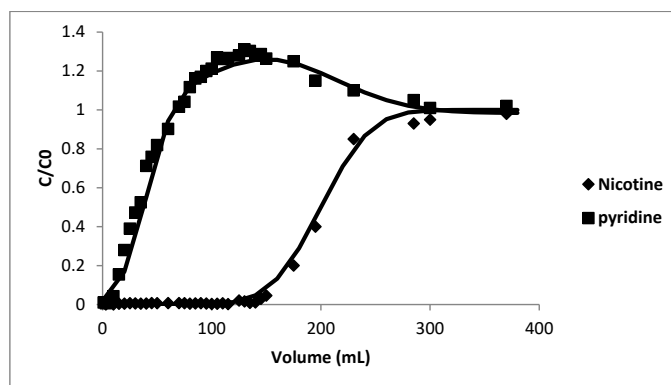|	Pyridine	Nicotine
Ce (mmol/L)	7.32	1.54
$q_{ad\ max}$ (mmol/g)	0.33	0.246
$q_{dés}$ (mmol/g)	0.254	-
q_{ad} (mmol/g)	0.076	0.246
RMSE	0.05	0.016
α(Nicotine/Pyridine)	3.2	

Fig. 10. Breakthrough curves of pyridine and nicotine removal (7.32mmol/L-1.54 mmol/L) by adsorption onto AM.

124

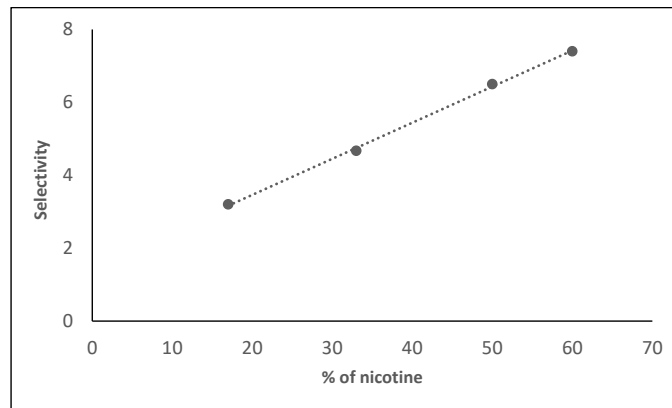*J. Water Environ. Nanotechnol., 5(2): 114-128 Spring 2020*

Fig. 11. Evolution of the selectivity (α Nicotine/pyridine) as a function of the nicotine molar (%).
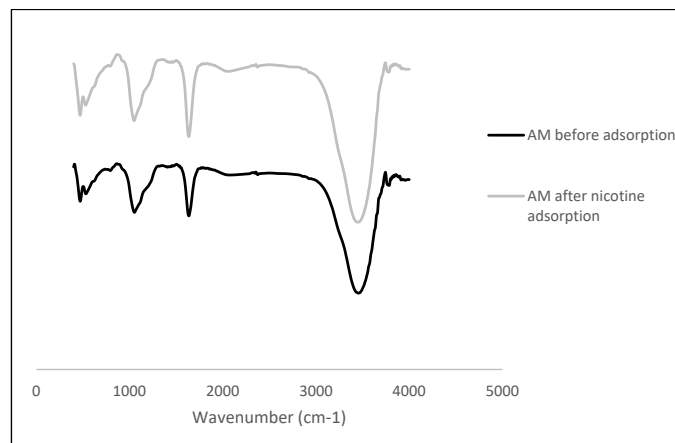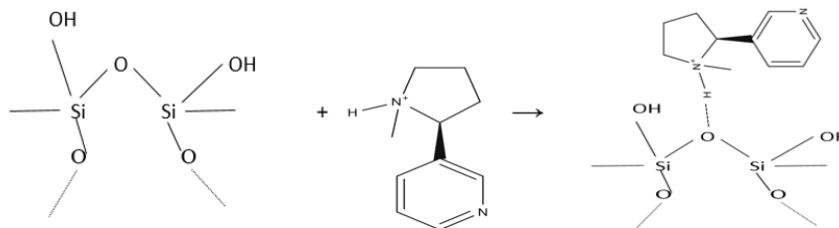

Fig. 12. FTIR spectra of activated Montmorillonite before and after nicotine adsorption.

adsorption; several peaks show a shift in the frequency of absorption bands. This is due to the interaction of the corresponding functional groups to nicotine. Shifts were observed for the bands corresponding to O-H bending from 3455 to 3450 ,Si–O bending from 1051 to 1046, Si–O–Al symmetrical stretching, from 531 and 469 to 527 and 466, indicating that nicotine interacts with Montmorillonite at Si–O sites. This indicates that nicotine was adsorbed principally by hydrogen bonding, according to the following reaction at pH = 6.3.

Regeneration of activated Montmorillonite

Desorption tests were conducted using an ethanol solvent. The desorption was conducted on spent adsorbent samples stemming from tests performed with an initial nicotine concentration of 6.2 mmol/L and adsorbent loading of 2 g. The spent adsorbents were desorbed by using a dynamic system until the total desorption of nicotine. After filtration and washing with deionized water, the solid was dried at room temperature and weighed. Consecutive adsorption-desorption cycles were
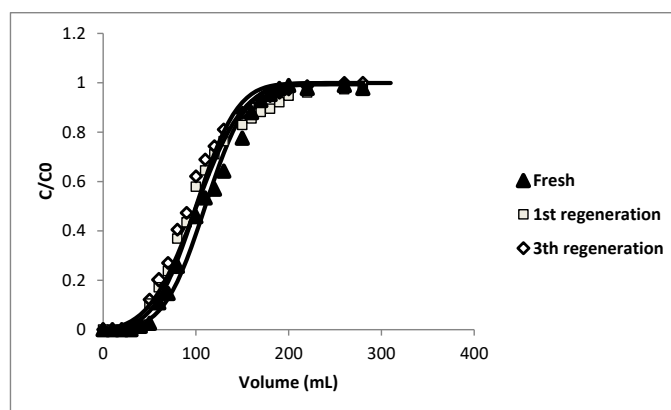
J. Water Environ. Nanotechnol., 5(2): 114-128 Spring 2020

125

Fig. 13. Breakthrough curves of nicotine on AM after 3 regeneration cycles.

Table 13. FTIR Bands for AM Alone and for AM after nicotine adsorption.

V cm^{-1}	Before adsorption	After adsorption
V O-H	3455	3450
V Si-O-Si	1051	1046
V Si-O-Al	531	527
V Si-O-Al	469	467

Table 14. Maximum adsorption capacity for the removal of nicotine by various adsorbents.

Adsorbent	Qads (mmol/g)	Reference
Activated Montmorillonite	0.68	This study
Activated carbon	1.75	Rakic et al [13]
Clinoptilolite	0.07	Rakic et al [13]
Mesoporous carbon	1.96	Cai et al [14]
Bentonite	0.236	Akcay et al [17]
Modified Montmorillonite	0.52	Ilić et al [40]
USY Zeolite	0.17	Lazarevic et al [41]
Hydrogel ME	0.166	Isikver et al [42]

also performed to study the regenerability and the stability of the activated Montmorillonite. These steps comprise the first adsorption-desorption cycle, which was followed by two more cycles using the same adsorbent. Fig. 13 shows the consecutive adsorption-desorption cycle data. As seen below, no significant loss (around 6%) of the adsorbent capacity was observed during three adsorption-desorption cycles. This demonstrates that the adsorbent was suitable for the design of a continuous sorption process.

Comparison of the nicotine adsorption capacity to different adsorbents

Table 14 shows the adsorption capacity at equilibrium for nicotine adsorption over different materials collected from the literature. The obtained value from our study is considerably higher or lower than those of some sorbent materials reported in the literature, Activated carbons are the most effective adsorbents for nicotine apparently due to their favorable surface properties. However, the activated carbon was partially regenerated under all the technics were used [43, 44]. There is thus our research is focused on Montmorillonite efficient and recyclable adsorbents.

CONCLUSION

In this study, a series of laboratory investigation was carried out to evaluate the dynamic and equilibrium adsorption studies on the removal of two organic compounds (nicotine and pyridine) from aqueous solution over activated Montmorillonite.

126

J. Water Environ. Nanotechnol., 5(2): 114-128 Spring 2020

The continuous adsorption system represented by the breakthrough curves depends on the initial concentration, the bed height, and the flow rate of the solution.

The experiments of Nicotine/pyridine mixtures lead to adsorption/desorption breakthrough curves. In this case, the pyridine was not adsorbed much in the AM, counter to Nicotine, which possesses the strongest interaction with the AM. These results revealed a higher affinity of nicotine adsorption than of pyridine on the AM.

The equilibrium adsorption capacities evaluated from the prepared solutions on dynamic conditions were slightly higher than those measured on a batch solution.

Electrostatic attraction and hydrogen bond interactions between adsorbate and adsorbent were the key mechanistic pathways for removal of nicotine and pyridine from wastewater

Regeneration tests using an ethanol solution were performed during three adsorption-desorption cycles. These results indicate that AM developed in this study was suitable for the design of a continuous sorption process.

SD: Supplementary Data is available for this article.

CONFLICT OF INTEREST

The authors declare that they have no conflict of interest.

REFERENCES

1. Benotti MJ, Brownawell BJ. Distributions of Pharmaceuticals in an Urban Estuary during both Dry- and Wet-Weather Conditions. Environmental Science & Technology. 2007;41(16):5795-802.
2. Alabi OA, Osifo-Whiskey E, Yadi P, Lawal M, Bakare AA. Tobacco Industry Wastewater^|^ndash;Induced Genotoxicity in Mice Using the Bone Marrow Micronucleus and Sperm Morphology Assays. CYTOLOGIA. 2014;79(2):215-25.
3. Anastopoulos I, Pashalidis I, Orfanos AG, Manariotis ID, Tatarchuk T, Sellaoui L, et al. Removal of caffeine, nicotine and amoxicillin from (waste)waters by various adsorbents. A review. Journal of Environmental Management. 2020;261:110236.
4. Novotny TE, Bialous SA, Burt L, Curtis C, Luiza da Costa V, Iqtidar SU, et al. The environmental and health impacts of tobacco agriculture, cigarette manufacture and consumption. Bulletin of the World Health Organization. 2015;93(12):877-80.
5. Mackie RS, Tscharke BJ, O'Brien JW, Choi PM, Gartner CE, Thomas KV, et al. Trends in nicotine consumption between 2010 and 2017 in an Australian city using the wastewater-based epidemiology approach. Environment International. 2019;125:184-90.
6. Buerge IJ, Kahle M, Buser H-R, Müller MD, Poiger T. Nicotine Derivatives in Wastewater and Surface Waters: Application as Chemical Markers for Domestic Wastewater. Environmental Science & Technology. 2008;42(17):6354-60.
7. da Silva CMF, Rocha QdC, Rocha PCS, Louvisse AMT, Lucas EF. Removal of naphthalene from aqueous systems by poly(divinylbenzene) and poly(methyl methacrylate-divinylbenzene) resins. Journal of Environmental Management. 2015;157:205-12.
8. Bayazit ŞS, Yildiz M, Aşçi YS, Şahin M, Bener M, Eğlence S, et al. Rapid adsorptive removal of naphthalene from water using graphene nanoplatelet/MIL-101 (Cr) nanocomposite. Journal of Alloys and Compounds. 2017;701:740-9.
9. Klamerth N, Malato S, Maldonado MI, Agüera A, Fernández-Alba AR. Application of Photo-Fenton as a Tertiary Treatment of Emerging Contaminants in Municipal Wastewater. Environmental Science & Technology. 2010;44(5):1792-8.
10. de Franco MAE, da Silva WL, Bagnara M, Lansarin MA, dos Santos JHZ. Photocatalytic degradation of nicotine in an aqueous solution using unconventional supported catalysts and commercial ZnO/TiO2 under ultraviolet radiation. Science of The Total Environment. 2014;494-495:97-103.
11. Tekle-Röttering A, Reisz E, Jewell KS, Lutze HV, Ternes TA, Schmidt W, et al. Ozonation of pyridine and other N-heterocyclic aromatic compounds: Kinetics, stoichiometry, identification of products and elucidation of pathways. Water Research. 2016;102:582-93.
12. Koubaissy B, Joly G, Magnoux P. Adsorption and Competitive Adsorption on Zeolites of Nitrophenol Compounds Present in Wastewater. Industrial & Engineering Chemistry Research. 2008;47(23):9558-65.
13. Rakić V, Damjanović L, Rac V, Stošić D, Dondur V, Auroux A. The adsorption of nicotine from aqueous solutions on different zeolite structures. Water Research. 2010;44(6):2047-57.
14. Antunes M, Esteves VI, Guégan R, Crespo JS, Fernandes AN, Giovanela M. Removal of diclofenac sodium from aqueous solution by Isabel grape bagasse. Chemical Engineering Journal. 2012;192:114-21.
15. Mansouri H, Carmona RJ, Gomis-Berenguer A, Souissi-Najar S, Ouederni A, Ania CO. Competitive adsorption of ibuprofen and amoxicillin mixtures from aqueous solution on activated carbons. Journal of Colloid and Interface Science. 2015;449:252-60.
16 Akçay, G., Yurdakoç, K.: Removal of nicotine and its pharmaceutical derivatives from aqueous solution by raw bentonite and dodecylammonium bentonite. Journal of Science and Industrial Research. 67, 451–454 (2008).
17. Gładysz-Płaska A, Lipke A, Tarasiuk B, Makarska-Białokoz M, Majdan M. Naphthalene sorption on red clay and halloysite modified by quaternary ammonium salts. Adsorption Science & Technology. 2017;35(5-6):464-72.
18. Wang C-J, Li Z, Jiang W-T, Jean J-S, Liu C-C. Cation exchange interaction between antibiotic ciprofloxacin and montmorillonite. Journal of Hazardous Materials. 2010;183(1-3):309-14.
19. Obi C, Okoye IP. Kinetic Evaluation of Naphthalene Removal using Acid - Modified and Unmodified Bentonite Clay Mineral. Journal of Applied Sciences and Environmental Management. 2014;18(1):143.
20. Ibrahim Z, Koubaissy B, Mohsen Y, Hamieh T, Daou TJ, Nouali H, et al. Adsorption of Pyridine onto Activated

J. Water Environ. Nanotechnol., 5(2): 114-128 Spring 2020

127

Montmorillonite Clays: Effect Factors, Adsorption Behavior and Mechanism Study. American Journal of Analytical Chemistry. 2018;09(10):464-81.

21. Li Z, Chang P-H, Jean J-S, Jiang W-T, Wang C-J. Interaction between tetracycline and smectite in aqueous solution. Journal of Colloid and Interface Science. 2010;341(2):311-9.

22. Sze MFF, Lee VKC, McKay G. Simplified fixed bed column model for adsorption of organic pollutants using tapered activated carbon columns. Desalination. 2008;218(1-3):323-33.

23. de Franco MAE, de Carvalho CB, Bonetto MM, Soares RdP, Féris LA. Removal of amoxicillin from water by adsorption onto activated carbon in batch process and fixed bed column: Kinetics, isotherms, experimental design and breakthrough curves modelling. Journal of Cleaner Production. 2017;161:947-56.

24. Pan B, Meng F, Chen X, Pan B, Li X, Zhang W, et al. Application of an effective method in predicting breakthrough curves of fixed-bed adsorption onto resin adsorbent. Journal of Hazardous Materials. 2005;124(1-3):74-80.

25. de Franco MAE, de Carvalho CB, Bonetto MM, de Pelegrini Soares R, Féris LA. Diclofenac removal from water by adsorption using activated carbon in batch mode and fixed-bed column: Isotherms, thermodynamic study and breakthrough curves modeling. Journal of Cleaner Production. 2018;181:145-54.

26. Borba CE, Silva EAd, Fagundes-Klen MR, Kroumov AD, Guirardello R. Prediction of the copper (II) ions dynamic removal from a medium by using mathematical models with analytical solution. Journal of Hazardous Materials. 2008;152(1):366-72.

27. Wolborska A. Adsorption on activated carbon of p-nitrophenol from aqueous solution. Water Research. 1989;23(1):85-91.

28. Wolborska A. External film control of the fixed bed adsorption. Chemical Engineering Journal. 1999;73(2):85-92.

29 Fowler, R. H., Guggenheim, E. A.: Statistical Thermodynamics, Theory of the Properties of Matter in Equilibrium, Cambridge University Press: New York (1965).

30. Koubaissy B, Toufaily J, El-Murr M, Jean Daou T, Hafez H, Joly G, et al. Adsorption kinetics and equilibrium of phenol drifts on three zeolites. Open Engineering. 2012;2(3).

31. Meng M, Feng Y, Zhang M, Liu Y, Ji Y, Wang J, et al. Highly efficient adsorption of salicylic acid from aqueous solution by wollastonite-based imprinted adsorbent: A fixed-bed column study. Chemical Engineering Journal. 2013;225:331-9.

32. Chen S, Yue Q, Gao B, Li Q, Xu X, Fu K. Adsorption of hexavalent chromium from aqueous solution by modified corn stalk: A fixed-bed column study. Bioresource Technology. 2012;113:114-20.

33. Futalan CM, Kan C-C, Dalida ML, Pascua C, Wan M-W. Fixed-bed column studies on the removal of copper using chitosan immobilized on bentonite. Carbohydrate Polymers. 2011;83(2):697-704.

34. Sabio E, Zamora F, Gañan J, González-García CM, González JF. Adsorption of p-nitrophenol on activated carbon fixed-bed. Water Research. 2006;40(16):3053-60.

35. Sotelo JL, Ovejero G, Rodríguez A, Álvarez S, García J. Analysis and modeling of fixed bed column operations on flumequine removal onto activated carbon: pH influence and desorption studies. Chemical Engineering Journal. 2013;228:102-13.

36. Lu Y, Jiang M, Wang C, Wang Y, Yang W. Impact of molecular size on two antibiotics adsorption by porous resins. Journal of the Taiwan Institute of Chemical Engineers. 2014;45(3):955-61.

37 Van-Vliet, B.M., Weber, W.J. Jr.: Comparative performance of synthetic adsorbents and activated carbon for specific compound removal from wastewaters. Journal Water Pollution Control Federation. 53, 1585-1598 (1981).

38. Koubaissy B, Joly G, Batonneau-Gener I, Magnoux P. Adsorptive Removal of Aromatic Compounds Present in Wastewater by Using Dealuminated Faujasite Zeolite. Industrial & Engineering Chemistry Research. 2011; 50(9):5705-13.

39. Ilic I, Jovic-Jovicic N, Bankovic P, Mojovic Z, Loncarevic D, Grzetic I, et al. Adsorption of nicotine from aqueous solutions on montmorillonite and acid-modified montmorillonite. Science of Sintering. 2019;51(1):93-100.

40. Lazarevic N, Adnadjevic B, Jovanovic J. Adsorption of nicotine from aqueous solution onto hydrophobic zeolite type USY. Applied Surface Science. 2011;257(18):8017-23.

41. Işikver Y, Ecevit T. Preparation and characterization of nicotine-selective hydrogels. Polymer Engineering & Science. 2016;56(9):1004-11.

42. Salvador F, Martin-Sanchez N, Sanchez-Hernandez R, Sanchez-Montero MJ, Izquierdo C. Regeneration of carbonaceous adsorbents. Part II: Chemical, Microbiological and Vacuum Regeneration. Microporous and Mesoporous Materials. 2015;202:277-96.

43. Boehler M, Zwickenpflug B, Hollender J, Ternes T, Joss A, Siegrist H. Removal of micropollutants in municipal wastewater treatment plants by powder-activated carbon. Water Science and Technology. 2012;66(10):2115-21.

128

J. Water Environ. Nanotechnol., 5(2): 114-128 Spring 2020